

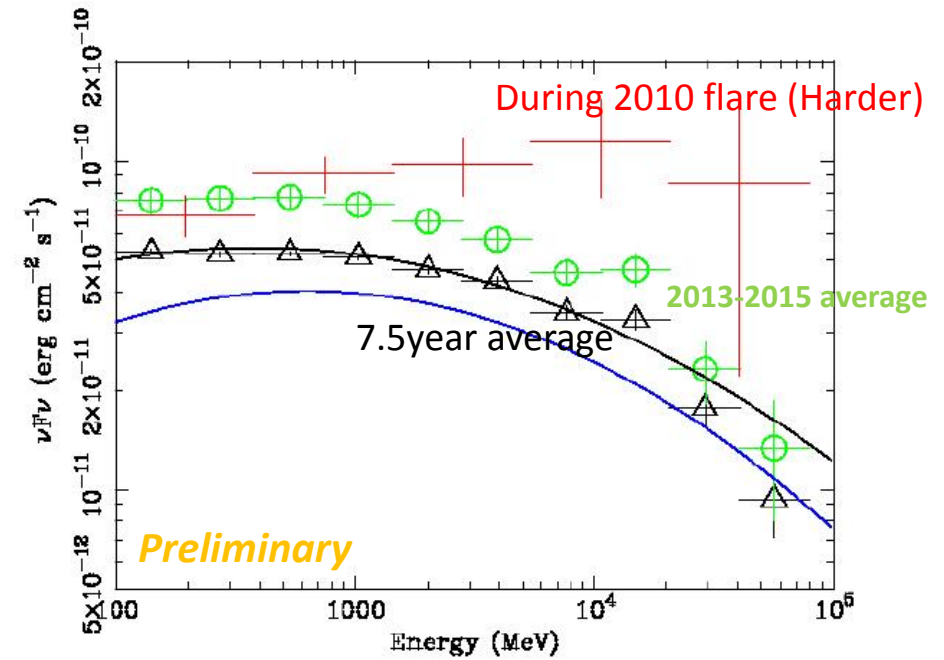
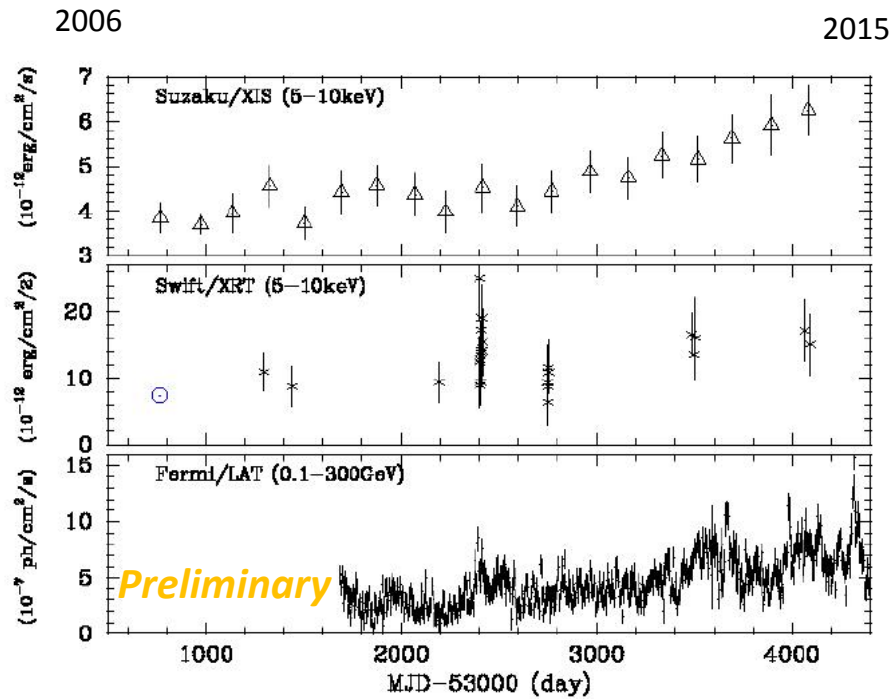
X-ray and GeV gamma-ray variability of the radio galaxy NGC 1275

Yasushi Fukazawa, Kensei Shiki, Fumiya Imazato (Hiroshima University), F. D'Ammando (INAF), R. Ojha (NASA/GSFC), and Fermi/LAT collaboration

Obtained light curves show a correlation between X-ray and GeV gamma-ray; we can see a long-term gradual increase in both X-ray and GeV. This is the first clear correlation between X-ray and GeV gamma-ray for NGC 1275. For the short-term variability, we do not find any clear correlation.

Fermi/LAT GeV gamma-ray spectra of NGC 1275. Black solid line represents the best-fit LogParabola model for the 7.5-yr, and blue solid line does for the 3FGL catalog (4 year).

LAT spectrum



1. Introduction

Radio Galaxies

Fermi-LAT detected 11 radio galaxies during the 1st year (Abdo+10, ApJ 720, 912). (21 in 3rd LAT catalog, Acero+15, ApJS 218, 23)

Radio galaxies are interesting and important for studying jet structures;
 Beaming is not so strong as typical blazars
 Emission from various sites can be observed; e.g. spine-sheath.

However, inner jet emission has been detected mainly in the radio and GeV gamma-ray band for most objects, due to bright stellar and accretion disk components in the optical and X-ray band; SED of jet emission is unclear.

In the paper, we report X-ray and gamma-ray studies of the GeV brightest radio galaxy NGC 1275, in order to disentangle the disk/corona and jet emission in the X-ray band.



Multiwavelength image of NGC1275

(X-ray: NASA/CXC/la/A.Fabian et al.; Radio: NRAO/VLA/G. Taylor; Optical: NASA, ESA, the Hubble Heritage (STScI/AURA)-ESA/Hubble Collaboration, and A. Fabian (Institute of Astronomy, University of Cambridge, UK))

☆ FR I radio galaxy NGC 1275

GeV gamma-ray brightest radio galaxy

BH mass: $3.4 \times 10^8 M_{\odot}$ (Wilman+05)

Redshift: 0.01756 (Strauss+92)

broad H α (~ 2750 km/s FWHM; Ho+97)

AGN jet-induced hot gas bubble in the Perseus cluster (Fabian+06)

Seyfert-like optical/X-ray spectra

GeV gamma-ray is significantly variable

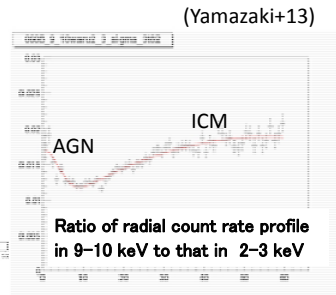
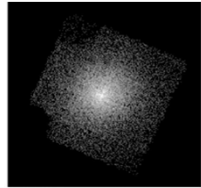
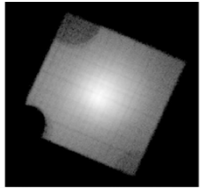
TeV gamma-ray has been detected several times

We analyzed all the archival X-ray data of Suzaku/XIS and Swift/XRT (2006-2015) to derive an X-ray light curve, and the Fermi/LAT GeV gamma-ray data (2008-2015) to study a correlation between X-ray and gamma-ray.

2. Suzaku/XIS data analysis

2-3 keV image

9-10 keV image

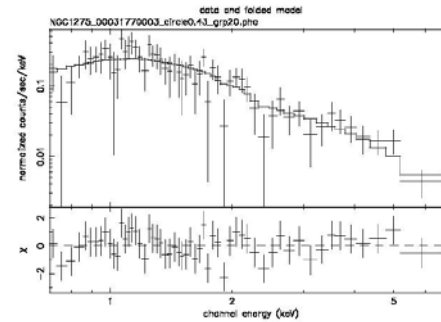


Suzaku observed NGC 1275 every half year for calibration. We analyzed all the archival XIS data in 2006-2015. As shown in the above images, X-ray emission mainly comes from extended intracluster medium (ICM) of the Perseus cluster. However, a point-like source was detected at the position of NGC 1275, and it can be seen that the point source is clear in the hard X-ray band. We performed imaging analyses in the same way as described in Yamazaki et al. (2013, PASJ 65, 30), as shown in the above. From the ratio of radial count rate profile between several energy bands, we obtained a spectrum of NGC 1275. The spectra are explained by a power-law with a photon index of 1.6-1.8. We estimated the X-ray flux from the obtained 18 spectra.

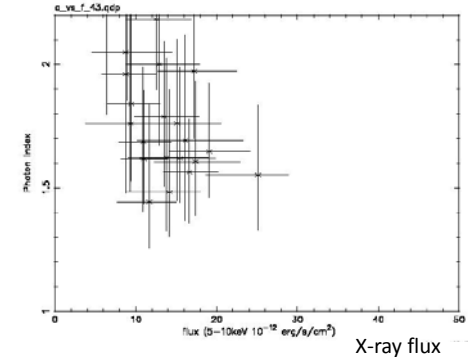
Yamasaki et al. (2013) reported no significant X-ray variability in 2006-2011. However, as shown in the below panels, we can see a gradual X-ray flux increase since 2013, and this trend is similar to the GeV gamma-ray flux increase.

3. Swift/XRT data analysis

PC mode data in 7-24 arcsec (MJD 55403)

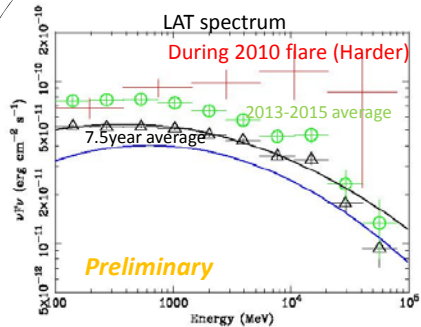


Photon index



We analyzed 25 observations in the PC mode. Some series of observations were followed by GeV gamma-ray flares. We extracted spectra within 7-24 arcsec from NGC 1275, to avoid the central pile-up region. Background spectra are taken from 60-61 arcsec from NGC 1275; note that ICM emission is also subtracted by these spectra. We fitted these spectra with a simple powerlaw with the Galactic absorption. As shown in the left panel, the power-law photon index is 1.4-2.0, with no clear correlation between flux and photon index.

4. Fermi/LAT data analysis

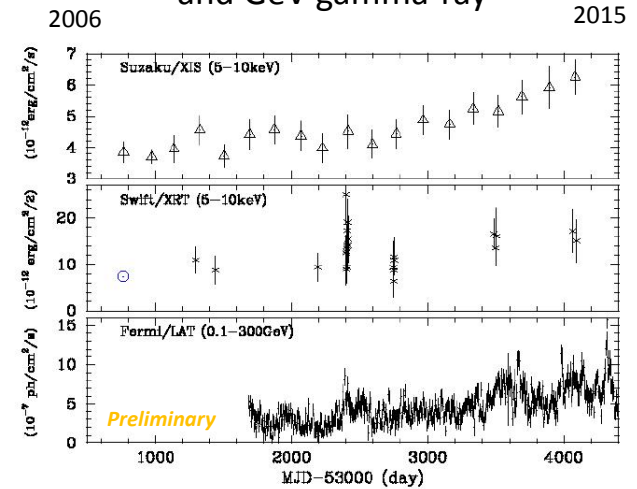


PASS-8 data (P8R2) (Atwood+13, ApJ 697, 1071)
 From Aug. 4, 2008 to Jan. 7th, 2016
 Source class events (event type 3, event class 128)
 Selected with a zenith angle cut of <90deg
 Time region : (DATA_QUAL>0)&&(LAT_CONFIG==1)
 Science Tools v10r0p5 with IRF P8R2_SOURCE_V6
 ROI: 22.5 radius
 Background point sources: from LAT 3rd catalog (Acero+15)
 Galactic diffuse: gll_iem_v06.fits (Acero+16, ApJS 223, 26)
 Instrumental residual background: iso_P8R2_SOURCE_V6_v06.txt

Fermi/LAT GeV gamma-ray spectra of NGC 1275. Black solid line represents the best-fit LogParabola model for the 7.5-yr, and blue solid line does for the 3FGL catalog (4 year).

We performed likelihood analysis. We derived the GeV gamma-ray light curve by binning the LAT data into 4-day bins and performing the gtlike analysis for each time bin. The power-law model is assumed for NGC 1275 emission. As a result, we obtained the GeV gamma-ray light curve as shown below. Next we derived the model-independent GeV gamma-ray spectrum by performing the likelihood analysis for 6 energy bands which are logarithmically spaced in 0.1--300 GeV. The derived spectra are shown in the above panels for three periods. The 7.5-yr spectrum has a higher flux than that in the 3FGL catalogue. The spectra of the 7.5-yr and high-flux periods have a similar shape with a curvature, peaking around 1 GeV and steepening toward the higher energy as reported by Aleksic+14 (ApJ A&A 564, A5). On the other hand, the spectrum during the 2010 flare is certainly harder and brighter than those of other periods.

5. Light curves of X-ray and GeV gamma-ray



Obtained light curves show a correlation between X-ray and GeV gamma-ray; we can see a long-term gradual increase in both X-ray and GeV. This is the first clear correlation between X-ray and GeV gamma-ray for NGC 1275. For the short-term variability, we do not find any clear correlation.

6 Discussion

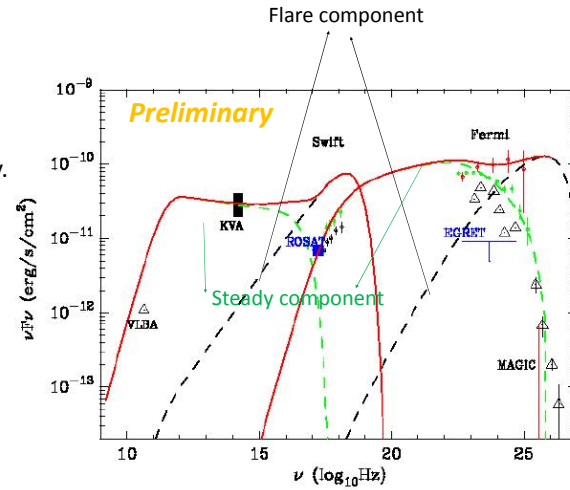
In the long-term variation, X-ray flux increase is not as large as GeV gamma-ray increase. Such behavior is reproduced by increase of the electron density, spectral hardening (decrease of electron energy distribution, increase of Doppler factor, and increase of magnetic field. However, the latter two cases are not consistent with a slight increase of optical flux in Aleksic et al. (2014, A&A 564, A5). Also, a year-scale gradual hardening of electron energy distribution is unlikely, since the cooling time of high energy electrons is much shorter than one year. Therefore, the increase of electron density is one possibility. In addition, the reduction of the size of the emission region, therefore the decrease of variable timescale may also contribute. We might see the jet collimation for the recent gradual brightening.

Short-term flares found with Swift/XRT coincides with GeV gamma-ray brightening for the flares in 2010 and 2013 (Brown&Adams+11 MNRAS 413, 2785; Ciprini+13 ATel 4753, 1}. This indicates that the source of the X-ray flare is the jet emission.

The 2010 flare showed a GeV gamma-ray flux increase by a factor of 2 with a spectral hardening. The synchrotron emission in the steady state does not reach the X-ray band (Abdo+09), and a stronger magnetic field could move the synchrotron cut-off to higher energy. However, the X-ray spectrum during the flare is not so steep and thus the synchrotron cut-off seems to exist in a higher energy band than the Swift/XRT band.

Therefore, in addition to the higher magnetic field, a higher maximum electron energy is needed. If the maximum electron energy increases by a factor of 10 in the flare, the synchrotron emission reaches the X-ray band. Shock-in-jet model can produce such a parameter change. If the flare is induced by the shock, the steep electron spectral index of 3.1 is not likely. Therefore, we calculate the SSC model by assuming a single power-law index of 2.0 and show the model curve in Figure (black dashed). Other parameters are summarized in table. In this case, the X-ray flare is almost dominated by the flaring synchrotron component,

while the hard gamma-ray emission is contributed by both a steady soft and a flaring hard SSC component.



	Base-line	steady	flare
Γ	2.3	same	same
B [G]	0.035	same	same
t_v [Ms]	13.4	8.94	0.80
p_1	2.1	same	2.0
p_2	3.1	same	2.0
γ_{\min}	8×10^2	same	same
γ_{\max}	4×10^5	same	4×10^6
γ_{brk}	9.6×10^2	same	same
$P_{j,B}$ [10^{40} erg s $^{-1}$]	0.24×10^4	0.11×10^4	8.7
$P_{j,e}$ [10^{40} erg s $^{-1}$]	2.0×10^4	3.0×10^4	2.6×10^3

Spectral energy distribution of NGC 1275: the VLBA radio data of the C3 component (Suzuki+12 ApJ 746, 140), optical KVA data (Aleksic+14). ROSAT/HXI flux (Fabian+15, MNRAS 451, 3061) (filled rectangular), Swift in the normal (black in 2007), high-flux (green in 2015), and flare (red) states (this work), the LAT and MAGIC gamma-ray data in the normal (black) state (Abdo+09 ApJ 699, 31;Aleksic+14), high-flux (green), and flare (red) states (this work). Solid red line represents the baseline parameter set, and other dashed lines are curves which are based on the parameter set where only one parameter (denoted one) is changed from the baseline parameter set. Right: Solid red line represents the double SSC model; one is for a steady component (green dashed) and the other is for a flare component (black dashed). See the table in detail.